ISSN 0006-2979, Biochemistry (Moscow), 2012, Vol. 77, No. 6, pp. 603-608. © Pleiades Publishing, Ltd., 2012.
Original Russian Text © T. V. Komarova, E. V. Sheval, D. V. Pozdyshev, V. S. Kolesnikova, Yu. L. Dorokhov, 2012, published in Biokhimiya, 2012, Vol. 77, No. 6, pp. 742-749.
Originally published in Biochemistry (Moscow) On-Line Papers in Press, as Manuscript BM12-026, April 22, 2012.

Rapid and Massive Green Fluorescent Protein Production Leads to Formation of Protein Y-Bodies in Plant Cells

T. V. Komarova[1,2], E. V. Sheval[1], D. V. Pozdyshev[1,2], V. S. Kolesnikova[1], and Yu. L. Dorokhov[1,2]*

[1]*Belozersky Institute of Physico-Chemical Biology, Lomonosov Moscow State University, 119991 Moscow, Russia; fax: (495) 939-3181*
[2]*Vavilov Institute of General Genetics, Russian Academy of Sciences, ul. Gubkina 3, 119991 Moscow, Russia; fax: (499) 132-8962; E-mail: dorokhov@genebee.msu.su*

Received February 10, 2012
Revision received February 25, 2012

Abstract—Although high level of recombinant protein production can be achieved via transient expression in plant cells, the mechanism by which tolerance to the presence of recombinant protein is acquired remains unclear. Here we show that green fluorescent protein (GFP) encoded by an intron-optimized tobacco mosaic viral vector formed large membraneless GFP bodies called Y-bodies that demonstrated mainly perinuclear localization. The Y-bodies were heterogeneous in size, approaching the size of the cell nucleus. Experiments with extracted GFP and live cell imaging showed that Y-bodies included actively fluorescent, non-aggregated, tightly packed GFP molecules. The plant cells probably formed Y-bodies to exclude the recombinant protein from normal physiological turnover.

DOI: 10.1134/S0006297912060065

Key words: *Agrobacterium tumefaciens*, green fluorescent protein (GFP), viral vector, Y-bodies, tobacco mosaic virus, transient expression

Agrobacterium-mediated transient gene expression provides a rapid alternative to the material- and time-consuming generation of stably transformed plants. This method provides synchronous gene expression because *Agrobacterium tumefaciens* is known to simultaneously infect at least 96% of cells in injected leaves [1]. The *Agrobacterium*-delivered first-generation *Tobacco mosaic virus* (TMV) vector has been hampered by low production capacity and required co-injection of plasmids encoding silencing suppressors [2-4]. Recently, a TMV vector using the MagnICON system was constructed [1, 5]. This system exploits intron-optimization of TMV-based cDNA, wherein putative cryptic splice sites were removed and multiple plant introns were inserted. MagnICON provides a very fast (expression requires only 3-4 days) and large protein yield (up to 80% of total soluble protein). Due to this optimization, the efficiency of vector RNA transport from the nucleus into the cytoplasm was increased.

Abbreviations: GFP, green fluorescent protein; IC, intermediate construct; Pr^{Act2}, *Arabidopsis thaliana act2* gene promotor; TMV, tobacco mosaic virus; MP, movement protein; PB, protein body; UTR, untranslated region.

* To whom correspondence should be addressed.

However, not only optimization of the vector, but also protein folding, localization, and stability influence the yield of the target product. Green fluorescent protein (GFP) has high stability and low conformational flexibility [6]. GFP is used not only as a tool for molecular imaging of proteins, but also as a carrier of vaccine antigens, facilitating their proper folding [4, 7]. Hydrophobic molecules such as elastin-like polypeptide [8], *Trichoderma reesei* hydrophobin HFBI [9], and Zera protein [10] can largely provide for accumulation of recombinant protein in plants and decrease risk of tissue necrosis [8]. Enhanced accumulation of GFP fused with such polypeptides in the plant cell is accompanied by formation of protein bodies (PBs) enclosed by endoplasmic reticulum derived membrane and localized in the cytoplasm. These organelles have similar size, morphology, and motility [8-10] and seem to be isolated depots of large amounts of heterologous protein in the cell.

Here we compared GFP production capacity of vectors based on TMV genome (the strain infecting members of *Brassicaceae* family) and showed that the intron-optimized TMV vector directed massive and accelerated GFP accumulation in *Nicotiana benthamiana* leaves that resulted in the formation of large fluorescent bodies called Y-bodies. In contrast to PBs, electron micrographs

suggest that Y-bodies are not surrounded by a membrane and are ultimately stored in the cytoplasm near the nuclear envelope. We found that Y-bodies contained actively fluorescent, non-aggregated, tightly packed functional GFP molecules.

MATERIALS AND METHODS

Plasmid constructs. The vector TMV(i):*GFP* was constructed in several cloning steps. To obtain the intermediate construct 1 (*IC1*) a fragment containing the *MP* gene 3′-region, *GFP*, 3′-UTR of TMV, and the transcription terminator *nos* was excised from the plasmid pICH4351 [5] using restriction endonucleases *Eco*RI and *Hind*III. This fragment was inserted into the plasmid pGEM3Z (Promega, USA). *IC2*. Replacement of *GFP* in IC1 for its intron-containing variant was performed at restriction sites of *Nco*I and *Bsr*GI. To prepare the final vector TMV(i):*GFP*, fragment 1 containing the *Arabidopsis thaliana act2* transcription promotor (Pr^{Act}), the TMV replicase gene with eight introns, and a portion of the *MP* gene was excised from the pICH17388 construct [11] at restriction sites of *Kpn*I and *Eco*RI. Fragment 2 was excised from IC2 using *Eco*RI and *Hind*III. Then fragments 1 and 2 were inserted in the binary vector pBIN19 treated with restriction endonucleases *Kpn*I and *Hind*III.

Plasmids pICH17388 and pICH4351, as well as the *GFP* gene containing the intron sequence, were kindly provided by Icon Genetics GmbH (Germany).

Visualization of GFP. GFP in *N. benthamiana* leaves was detected using a UV lamp, $\lambda = 366$ nm, 2-5 days after agroinfiltration.

Confocal microscopy and estimation of GFP motility. Microscopy was carried out using an LSM510 confocal laser scanning microscope (Zeiss, Germany). GFP was photoactivated with a short pulse (~0.5 sec) at maximum laser power. Living cells were observed at 1% maximum power of the laser. Curves were obtained on the basis of images after subtraction of background. Relative fluorescence intensity (*RFI*) of the cell was calculated according to the equation: $RFI = T_0 I_t / T_t I_0$, where T_0 is overall intensity of the cell fluorescence before bleaching, T_t – overall intensity of the cell fluorescence at time t, I_0 – the mean intensity in the area of interest during prebleach, and I_t – the mean intensity in the area of interest at time t. The data were processed using the AutoFRAP plug-in (http://cellbiol.genebee.msu.ru/research.html) for ImageJ (NIH, USA).

Electron microscopy. Leaf fragments were fixed with 4% glutaraldehyde (Pelco, Russia) solution in 0.1 M Sorensen's sodium phosphate buffer, pH 7.4, for 2 h followed by post-fixation with 1% OsO_4 for 1.5 h and embedded in Epon 812 epoxide resin (Fluka, USA). Ultrathin sections were prepared using an LKB Ultratome III (LKB, USA). The sections were contrasted with uranyl acetate and lead nitrate and analyzed on an H700 electron microscope (Hitachi, Japan). For staining with antibodies against GFP, the leaf material was fixed with solution containing 2% formaldehyde and 0.1% glutaraldehyde and embedded in LR White (Sigma). Ultrathin sections were placed onto nickel grids with formvar support film and incubated in 20 mM glycine solution (30 min) and 1% BSA (60 min) to prevent unspecific antibody binding. The sections were sequentially incubated on drops with anti-GFP gold-conjugated antibodies (Sigma) followed by removal of unbound antibodies with 1× PBS. The sections were counterstained with uranyl acetate and examined under the electron microscope.

Preparation of plant extracts and analysis of proteins by SDS-PAGE. Total soluble protein from infiltrated leaves was extracted with 10 mM Tris-HCl buffer, pH 8.0, containing 200 mM NaCl (GFP buffer). Plant tissue (100 mg) was homogenized in 400 µl of GFP buffer with addition of Celite, followed by centrifugation at 16,000*g* for 5 min; then 50 µl of 4× sample buffer (200 mM Tris-HCl, pH 6.8, containing 40% glycerol, 4% SDS, 200 mM 2-mercaptoethanol, and 0.005% Bromophenol blue) was added to 150 µl of the supernatant. The supernatant (200 µl) was used for quantification of soluble GFP: its volume was adjusted to 1 ml, and fluorescence was measured on a QUANTECH fluorimeter (Barnstead International, USA) using the filters NB390 (excitation) and NB520 (emission). The volume of preliminarily prepared sample applied onto a polyacrylamide gel was determined from the GFP fluorescence intensity, so that GFP amounts (relative fluorescence units) were equal in all samples. PAGE of equalized samples was carried out before or after heat treatment (95°C, 5 min). GFP in polyacrylamide gel was visualized using a UV lamp emitting at $\lambda = 366$ nm.

RESULTS

TMV-based intron-containing vector provides massive accumulation of GFP in plant cells. Using agroinfiltration, we compared two vectors based on the TMV genome (the strain infecting members of *Brassicaceae* family), TMV:*GFP* (pICH4351) [5] (Fig. 1a) and its intron-containing analog TMV(i):*GFP* (Fig. 1b). The data presented in Fig. 1c demonstrate dynamics of GFP accumulation in leaf zones infiltrated with each of the vectors, TMV:*GFP* (*1*) and TMV(i):*GFP* (*2*). One can see that TMV(i):*GFP* provides faster and more intensive production of GFP in cells (Fig. 1c). Leaf fluorescence under the UV lamp was not observed on the 2nd day after agroinfiltration (Fig. 1c). Nevertheless, small GFP-containing structures were revealed by confocal fluorescence microscopy of epidermal cells transformed with

TMV(i):*GFP* (Fig. 1d). These structures considerably increased in size on the 3rd day, and fluorescence of the zone agroinfiltrated with TMV(i):*GFP* became visible under UV illumination (Fig. 1c). GFP-containing structures resembled inclusion bodies found by Ivanowski in tobacco leaves infected with TMV [12] and later named X-bodies [13, 14]. The non-intronized vector TMV:*GFP* only provided detectable GFP production on the 4th day (Fig. 1c) and did not lead to formation of any GFP aggregates in the infiltrated leaves. Only uniform fluorescence of cytoplasm was observed under a microscope in these leaves (data not shown).

We named the GFP aggregates, which were revealed after cell infiltration with TMV(i):*GFP*, Y-bodies and concluded that the TMV-based intronized vector provides massive accumulation of GFP in the plant cell accompanied by Y-body formation.

Characterization of observed Y-bodies and dynamic characteristics of GFP in the living cell. Morphological features of the observed Y-bodies were evaluated by confocal laser scanning microscopy. Numerous small (0.5-5 μm) inclusion bodies were already found in epidermal cells of leaves infiltrated with TMV(i):*GFP* on the 2nd day after infiltration (Fig. 2a, left). Their size increased to 10-20 μm on the 3rd day (Fig. 2a, right). Both size and number of Y-bodies increased with time. This led us to conclusion that large structures appeared due to the growth of small bodies and their subsequent merge (Fig. 2b, upper photo). It is worth noting that aggregation was not observed in mesophyll cells, in which only small inclusion bodies were observed both on the 2nd and 3rd days (Fig. 2b, lower photo). This can be explained by the hypothesis that chloroplasts create some spatial barrier counteracting merging. It should be emphasized that Y-bodies were not found in cells transformed with the intronless vector TMV:*GFP*: on the 3rd and 4th days after agroinfiltration GFP was uniformly distributed in the cytoplasm (data not shown).

Stable structures can be formed by highly mobile proteins [15]. To estimate dynamic parameters of GFP in observed Y-bodies in a living cell, we used the method of photoactivation. The essence of this method is that a distinct area of living cell is irradiated by a powerful laser spot pulse causing elevation of fluorescence in the area of choice (Fig. 2c). The rate of initial fluorescence level restoration and changes in fluorescence level in surrounding spots allow estimation of the dynamics of protein molecules distribution. In our case, fluorescence did not decrease for 70 sec (Fig. 2, c and d), which is indicative of the stability of GFP in Y-bodies and absence of the pro-

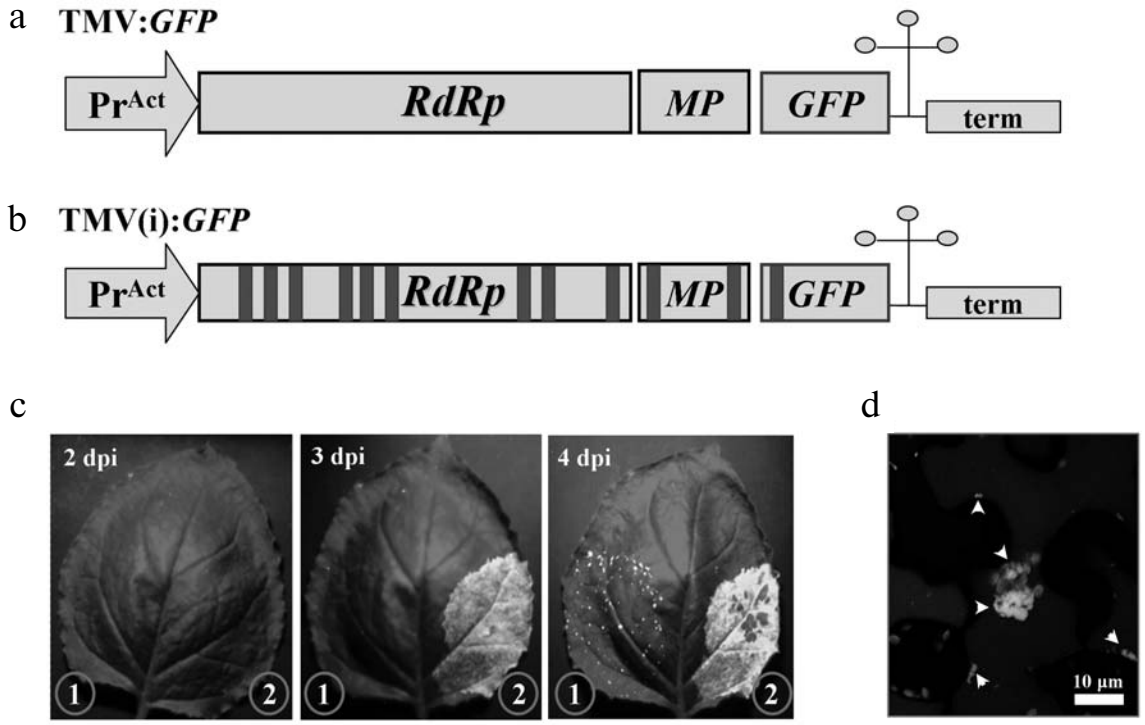

Fig. 1. TMV-based intron-containing vector provides massive GFP production. Schematic representation of the TMV-based vector TMV:*GFP* (a) and its intron-containing variant TMV(i):*GFP* (b). Pr^{Act2}, *Arabidopsis thaliana act2* gene promotor; *RdRp*, replicase gene; *MP*, movement protein gene; *GFP*, green fluorescent protein gene; term, transcription terminator; introns are denoted by dark-gray rectangles. c) UV visualization of GFP in leaves infiltrated with TMV:*GFP* (left part of the leaf, *1*) and TMV(i):*GFP* (right part of the leaf, *2*) on the 2nd, 3rd, and 4th days after infiltration. d) Image of epidermal cells of leaves infiltrated with TMV(i):*GFP*, 3rd day; UV illumination. Arrows indicate zones of GFP accumulation (Y-bodies).

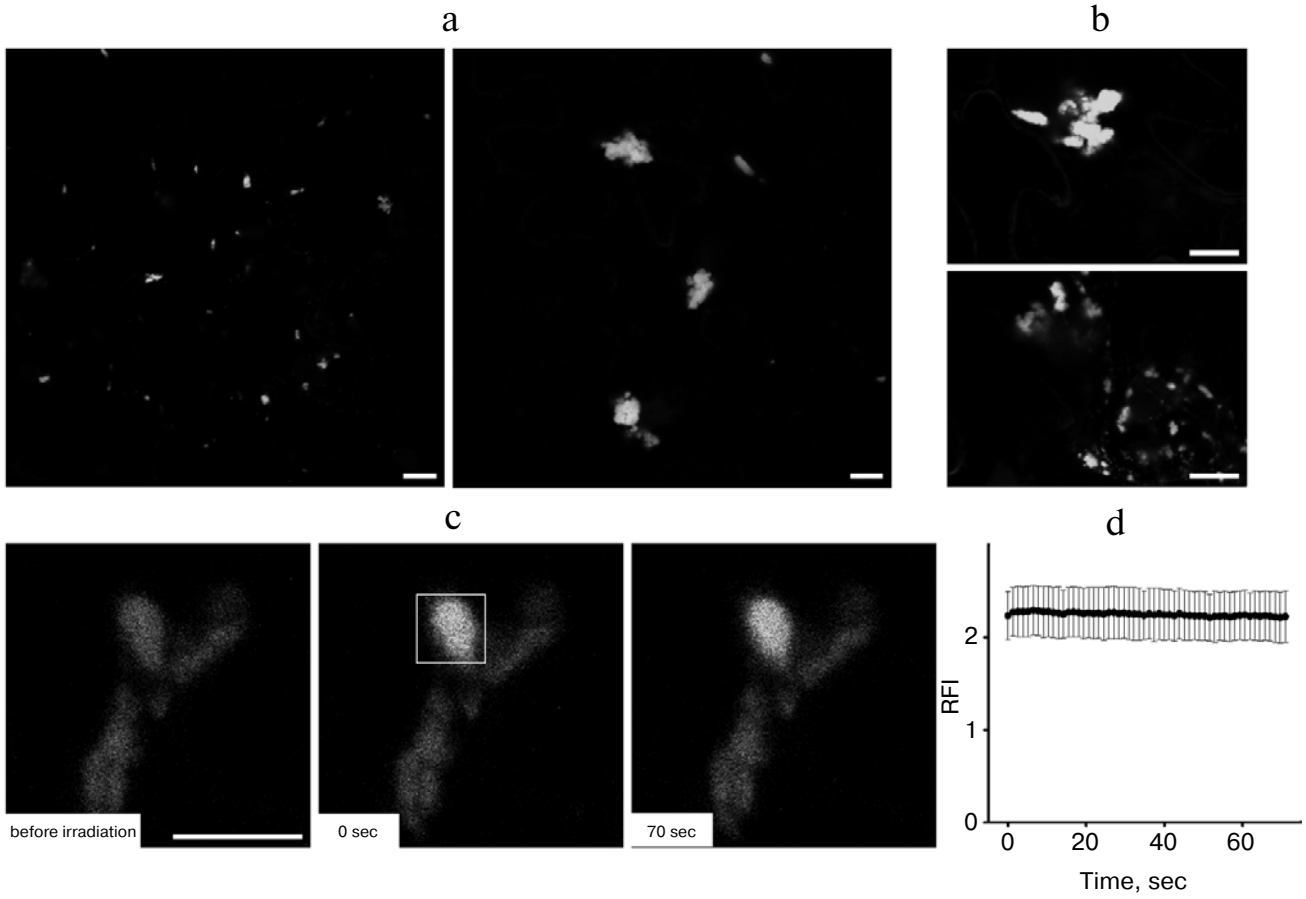

Fig. 2. Morphology and localization of GFP-containing Y-bodies. a) Size and structure of GFP-containing Y-bodies in epidermal cells of the leaf 2 (left photo) and 3 (right photo) days after infiltration with the vector TMV(i):*GFP*. b) Size and localization of GFP-containing Y-bodies in cells of epidermis (upper photo) and mesophyll (bottom photo) on the 3rd day after agroinfiltration with the vector TMV(i):*GFP*. c) Photoactivation study of GFP mobility in Y-bodies. The cells expressing GFP were photographed before and after photoactivation of fluorescent proteins (a large Y-body is framed). Scale, 10 μm. d) Quantitative estimation of GFP mobility. No change in relative fluorescence suggests low mobility of the protein comprising the GFP-containing bodies. RFI, relative fluorescence intensity.

tein exchange between the observed structures and cytoplasm.

Analysis of GFP-containing Y-body morphology by electron microscopy. Electron microscopy confirmed the presence of electron-dense homogeneous structures in both epidermal and mesophilic cells on the 3rd day after agroinfiltration with TMV(i):*GFP* (Fig. 3a). Using gold-labeled antibodies against GFP, we demonstrated that these structures contain green fluorescent protein (Fig. 3b), while other areas remain unstained, which is consistent with the data of fluorescence microscopy. The size of the GFP-containing Y-bodies varied greatly, achieving 10-20 μm in diameter (in the epidermal cells). The largest Y-bodies were localized in the vicinity of the cell nucleus and were probably composed of smaller granules (Fig. 3a). High-resolution analysis revealed that Y-bodies are not surrounded by a membrane.

Y-Bodies do not contain aggregated GFP molecules. Aggregation is known to be a common phenomenon in overexpression of recombinant proteins in both bacterial and eukaryotic cells. To visualize aggregation of purified GFP, we used "pseudo-native" protein electrophoresis [16] based on discontinuous SDS-PAGE of non-heated protein samples. Under these conditions, GFP not only retains fluorescent properties, but oligomers migrate as high molecular weight bands [17]. Total soluble protein was extracted from leaves agroinfiltrated with either TMV(i):*GFP* or TMV:*GFP*, on the 4th day after infection. To load equal amounts of GFP onto the gel, we measured GFP fluorescence of soluble protein extracts and loaded an equal amount of relative fluorescence units on the gels before or after heat treatment (95°C, 5 min). Figure 4 demonstrates that in the gel the extract of leaves agroinfiltrated with TMV(i):*GFP* gives a fluorescing band corresponding to ~27 kDa (lanes *1* and *2*), i.e. to the molecular weight of the GFP monomer. There is neither supermolecular structure at the top of the gel nor oligomers migrating as high molecular weight bands. The samples

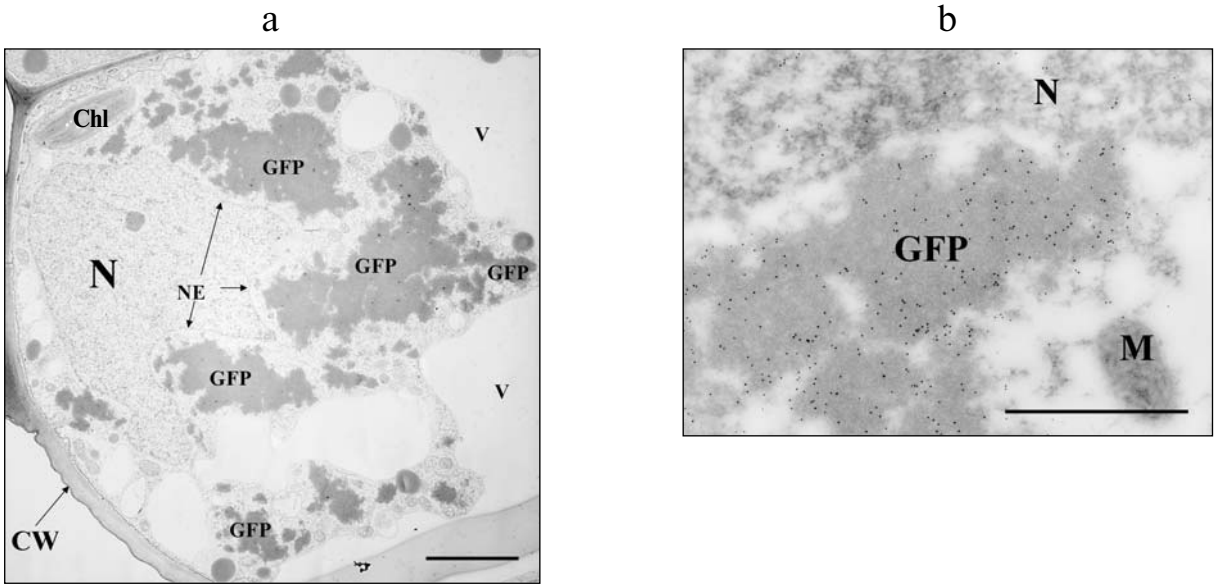

Fig. 3. Morphology of cells with GFP-containing Y-bodies. a) Electron microphotography of *N. benthamiana* epidermal cells infiltrated with TMV(i):*GFP*. Third day after infiltration. N, nucleus; NE, nuclear envelope; Chl, chloroplast; CW, cell wall; V, vacuole. Scale, 3 μm. b) Electron microphotography of epidermal cell stained with gold-labeled antibodies against GFP. N, nucleus; M, mitochondrion. Scale, 1.5 μm.

from the leaves agroinfiltrated with TMV:*GFP* gave less intense fluorescing bands (lanes *3* and *4*). Heating of samples (95°C, 5 min) resulted in loss of fluorescence in both sample types (lanes *5*, *6* and *7*, *8*). SDS-PAGE of protein extracts showed different fluorescence intensity of GFP bands for TMV(i):*GFP* and TMV:*GFP*, despite preliminary equalization of the samples by fluorescence of soluble GFP. We conclude that a considerable part of the GFP comprising Y-bodies is shielded against excitation or emission and is not detected in solution, whereas SDS causes partial "unfolding" of Y-bodies and, as a consequence, 6-10-fold elevation of GFP fluorescence in the gel in the case of TMV(i):*GFP* compared to that of TMV:*GFP* (Fig. 4, compare the lanes *1*, *2* and *3*, *4*). Nevertheless, Y-bodies probably do not contain GFP oligomers and aggregates.

DISCUSSION

Plant cells have protein quality control mechanisms that serve to constantly monitor the quality of newly synthesized proteins and to actively remove unfolded or misfolded proteins [18-20]. On the other hand, plant cells are adapted to the accumulation of multiple copies of protein molecules. Through the course of evolution, higher plants have developed the ability to store proteins in a stable form in their seeds. Storage proteins accumulate in specialized vacuoles called protein storage vacuoles, which are membrane-bound organelles and essentially comprise an enclosed subcellular compartment [21]. This cellular process has turned out to be useful for increasing the accumulation of recombinant proteins fused with hydrophobic peptides. These peptides, such as elastin-like polypeptide [8], hydrophobin [9], and Zera protein [10] induce formation of inclusion bodies surrounded by endoplasmic membrane. Substantial elevation of the accumulation level in plant cells and decrease in necrosis

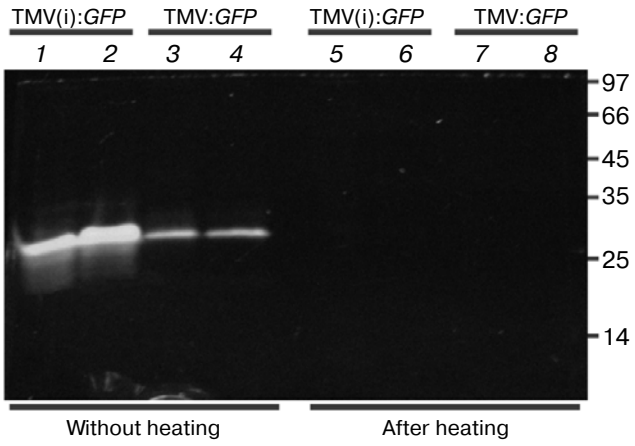

Fig. 4. Y-Bodies do not contain GFP aggregates. Total soluble protein was isolated from *N. benthamiana* leaves on the 4th day after infiltration with either TMV(i):*GFP* or TMV:*GFP*. Samples in buffer containing SDS – either without heating (lanes *1-4*) or after heating at 95°C for 5 min (lanes *5-8*) – were loaded into SDS-polyacrylamide gel. The GFP-containing bands were visualized using UV illumination.

of transformed tissues are observed for recombinant proteins conjugated with these peptides [9].

TMV infection of tobacco cells under natural conditions leads to accumulation of a large amount of coat protein and mature viral particles, which form inclusions seen in epidermal cells even under a light microscope. Ivanowski was the first investigator who observed these inclusions in 1903 [12]. Detailed study of these structures later called X-bodies [13, 14] under an electron microscope revealed clustering of mature TMV particles lying free in the cytoplasm and, unlike the storage proteins, not surrounded by membrane structures [13]. It is worth noting that the TMV particle contains 95% coat protein, so a comparison is relevant between X-bodies and protein storage organelles. However, unlike these organelles, the TMV X-bodies are not surrounded by membrane.

We have shown in the present work that the TMV-based intron-containing vector provides rapid and massive accumulation of GFP in *N. benthamiana* leaves, leading to formation of GFP-containing novel structures that we have called Y-bodies. Unlike the TMV X-bodies, they contain protein but not mature viral particles.

The size and number of the novel structures, Y-bodies, tended to increase with time, which suggested growth and subsequent merging at 3 days after infiltration (Fig. 2). The largest Y-bodies, reaching 10-20-μm size (Fig. 2, a and b), were located close to cell nuclei, and GFP presence was confirmed by immunogold labeling (Fig. 3b). In contrast to storage vacuoles and PBs, the Y-bodies were not surrounded by membranes. The photoactivation approach (Fig. 2, b and c) showed that the GFP molecules were bound stably within the Y-body and had no significant exchange with the surrounding cytoplasm. The mechanism of Y-body formation is unclear but the concept of protein self-organization [15, 22] may be useful in explaining this phenomenon. We can conclude from this study that the formation of Y-bodies leads to the exclusion of recombinant protein from normal physiological turnover.

Authors are grateful to Y. Gleba and V. Klimyuk (IconGenetics GmbH, Germany) for kindly provided plasmids and E. P. Senchenkov, A. V. Lazarev, and M. Yu. Mogilnikov for technical support.

This study was supported by the Russian Foundation for Basic Research (grant Nos. 11-04-01152-a (T.V.K) and 12-04-01237-a (E.V.Sh.)), Optek Ltd. (E.V.Sh.), and the Federal Targeted Program (state contract Nos. 16.512.11.2268 (Yu.L.D.) and 16.512.11.2279 (Yu.L.D.)).

REFERENCES

1. Marillonnet, S., Thoeringer, C., Kandzia, R., Klimyuk, V., and Gleba, Y. (2005) *Nat. Biotechnol.*, **23**, 718-723.
2. Dorokhov, Y. L., Sheveleva, A. A., Frolova, O. Y., et al. (2007) *Tuberculosis (Edinb.)*, **87**, 218-224.
3. Azhakanandam, K., Weissinger, S. M., Nicholson, J. S., Qu, R., and Weissinger, A. K. (2007) *Plant Mol. Biol.*, **63**, 393-404.
4. Lacorte, C., Lohuis, H., Goldbach, R., and Prins, M. (2007) *Virus Res.*, **129**, 80-86.
5. Marillonnet, S., Giritch, A., Gils, M., Kandzia, R., Klimyuk, V., and Gleba, Y. (2004) *Proc. Natl. Acad. Sci. USA*, **101**, 6852-6857.
6. Hsu, S. T., Blaser, G., and Jackson, S. E. (2009) *Chem. Soc. Rev.*, **38**, 2951-2965.
7. Huang, Z., Chen, Q., Hjelm, B., Arntzen, C., and Mason, H. (2009) *Biotechnol. Bioeng.*, **103**, 706-714.
8. Conley, A. J., Joensuu, J. J., Menassa, R., and Brandle, J. E. (2009) *BMC Biol.*, **7**, 48.
9. Joensuu, J. J., Conley, A. J., Lienemann, M., Brandle, J. E., Linder, M. B., and Menassa, R. (2010) *Plant Physiol.*, **152**, 622-633.
10. Torrent, M., Llompart, B., Lasserre-Ramassamy, S., Llop-Tous, I., Bastida, M., Marzabal, P., Westerholm-Parvinen, A., Saloheimo, M., Heifetz, P., and Ludevid, M. D. (2009) *BMC Biol.*, **7**, 5.
11. Giritch, A., Marillonnet, S., Engler, C., van Eldik, G., Botterman, J., Klimyuk, V., and Gleba, Y. (2006) *Proc. Natl. Acad. Sci. USA*, **103**, 14701-14706.
12. Ivanowski, D. (1903) *Z. Pflanzenkr. Pflanzenschutz*, **13**, 1-41.
13. Esau, K., and Cronshaw, J. (1967) *J. Cell. Biol.*, **33**, 665-678.
14. Hills, G. J., Plaskitt, K. A., Young, N. D., Dunigan, D. D., Watts, J. W., Wilson, T. M., and Zaitlin, M. (1987) *Virology*, **161**, 488-496.
15. Misteli, T. (2008) *Nature*, **456**, 333-334.
16. Baird, G. S., Zacharias, D. A., and Tsien, R. Y. (2000) *Proc. Natl. Acad. Sci. USA*, **97**, 11984-11989.
17. Yanushevich, Y. G., Staroverov, D. B., Savitsky, A. P., Fradkov, A. F., Gurskaya, N. G., Bulina, M. E., Lukyanov, K. A., and Lukyanov, S. A. (2002) *FEBS Lett.*, **511**, 11-14.
18. Hartl, F. U., and Hayer-Hartl, M. (2002) *Science*, **295**, 1852-1858.
19. Hatakeyama, S., and Nakayama, K. I. (2003) *J. Biochem.*, **134**, 1-8.
20. Esser, C., Alberti, S., and Hohfeld, J. (2004) *Biochim. Biophys. Acta*, **1695**, 171-188.
21. Robinson, D. G., Oliviusson, P., and Hinz, G. (2005) *Traffic*, **6**, 615-625.
22. Misteli, T. (2001) *J. Cell Biol.*, **155**, 181-185.